JOURNAL OF Applied Polymer SCIENCE

Thermal conductivity and electromagnetic shielding effectiveness of composites based on Ag-plating carbon fiber and epoxy

Junpeng Li, Shuhua Qi, Mengyu Zhang, Zhaofu Wang
Department of Applied Chemistry, School of Science, Northwestern Polytechnical University, Xi'an 710072, China
Correspondence to: S. Qi (E-mail: qishuhua@nwpu.edu.cn)

ABSTRACT: Thermally conductive and electromagnetic interference shielding composites comprising low content of Ag-plating carbon fiber (APCF) were fabricated as electronic packing materials. APCF as conductive filler consisting of carbon fiber (CF) employed as the structural component to reinforce the mechanical strength, and Ag enhancing electrical conductivity, was prepared by advanced electroless Ag-plating processing on CF surfaces. Ag coating had a thickness of 450 nm without oxide phase detected. The incorporation of 4.5 wt % APCF into epoxy (EP) substrate yielded thermal conductivity of 2.33 W/m·K, which is approximately 2.6 times higher than CF–EP composite at the same loading. The APCF–EP composite performed electromagnetic shielding effectiveness of 38–35 dB at frequency ranging from 8.2 to 12.4 GHz in the X band, and electromagnetic reflection was the dominant shielding mechanism. At loading content of APCF up to 7 wt %, thermal conductivity of APCF–EP composites increased to 2.49 W/m·K. Volume resistivity and surface resistivity decreased to 9.5×10^3 Ω·cm and 6.2×10^2 Ω, respectively, which approached a metal. © 2015 Wiley Periodicals, Inc. J. Appl. Polym. Sci. **2015**, *132*, 42306.

KEYWORDS: composites; fibers; thermal properties

Received 21 December 2014; accepted 4 April 2015
DOI: 10.1002/app.42306

INTRODUCTION

With further miniaturization of modern microelectronics, heat dissipation has been critical to device performance, reliability and life span since high integration of electronic components has resulted in the escalation of power consumption and heat accumulation.[1–3] As well as electromagnetic interference (EMI) is another important technical requirement for the modern integrated circuits, which emits severe electromagnetic radiation, and interferes with sensitive precision electronic devices. In order to address the aforementioned problems, an electronic packing material coupling with thermal conductivity and EMI shielding is urgent.

Great efforts have been made for the development of high-performance thermally conductive materials.[4–7] Recently much attention has been paid on polymer substrate composites. Compared with metallic and ceramic materials, polymer composites possess the advantages of light weight, high corrosion resistance and easy processability.[8,9] Usually, thermal conductivity of polymer composites has been enhanced by the addition of thermally conductive fillers, such as carbon-based fillers, metallic fillers and ceramic fillers.[10–13] With regard to EMI shielding effectiveness (SE), it is believed that high electrical conductivity benefits EMI shielding performance.[14,15] The loading with metallic particles may result in electrical conductivity. However, the density increases when significant metal addition to polymer matrix, thus limiting application when lightweight is required. Carbon-based fillers appear to be the promising fillers coupling electrical conductivity and lightweight. To improve electrical conductivity, a high content and well dispersion are required to form conductive networks. Short carbon fiber (CF) at a low loading content is easily dispersed into polymer matrix under mechanical stirring or ultrasonic. Additionally, short CF is highly isotropic, which benefits uniform heat dissipation in the direction parallel to heat flux.[16,17] However, CF shows lower electrical conductivity than metal. High CF loading content causes severe agglomeration and poor filler–matrix bonding, which deteriorate the mechanical property and processibility.[16,17]

Ag with excellently thermal and electrical conductivity, antioxidant and anticorrosion is welcome as a material for deposit coating. Plenty of Ag-plating process researches have appeared.[18–21] Ag-plating process on CF surface can be applied to improve the CF surface conductivity, so as to enhance the EMI shielding performance of composites with a low loading content. To the best of the authors' knowledge, there has been

Additional Supporting Information may be found in the online version of this article.

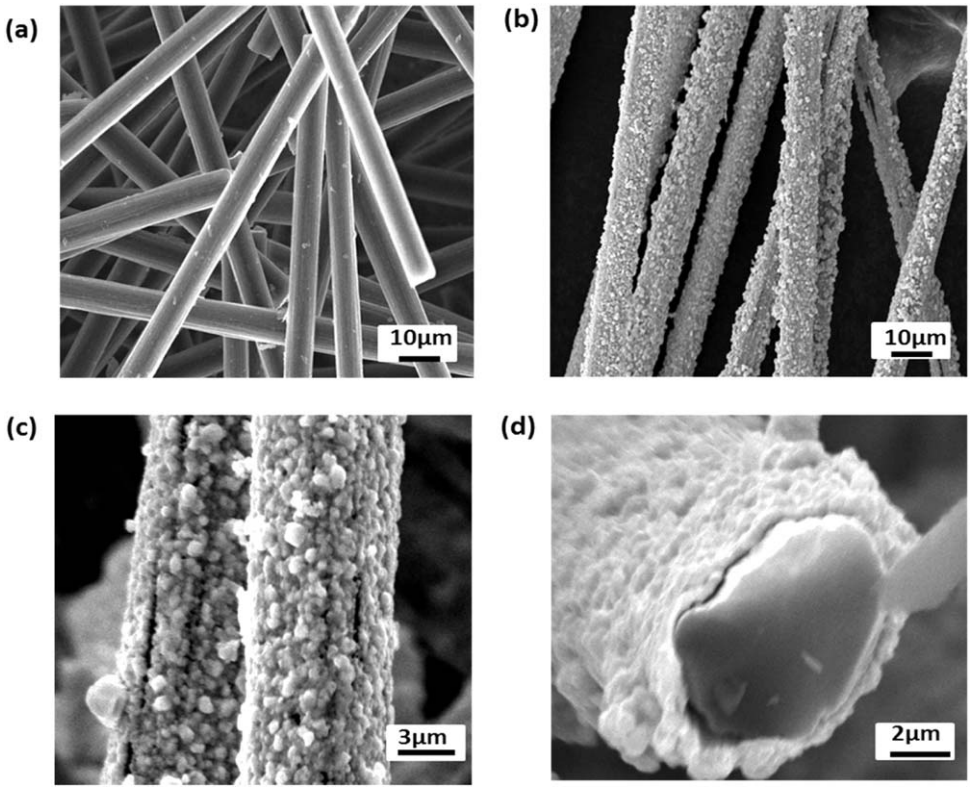

Figure 1. SEM images of (a) CF, (b, c) APCF, and (d) cross-sectional APCF.

few report about thermal conductivity and electromagnetic SE of polymer composite filled with Ag-plating short CF applied for electronic packing.

Herein, in this research a lightweight thermally conductive and electromagnetic shielding epoxy (EP) composite comprising low content of conductive Ag-plating carbon fiber (APCF) as fillers was fabricated as the electronic packing materials. APCF was prepared by electroless plating method on the surface of short CF. SEM images show CF was wrapped by Ag coating completely without Ag oxide phase detected in XRD and EDS. APCF-EP composite with loading content of 4.5 wt % exhibited thermal conductivity of 2.33 W/m·K and EMI shielding effectiveness of 38–35 dB at frequency ranging from 8.2 to 12.4 GHz in the X band. In addition, mechanical property and thermal stability were improved significantly.

EXPERIMENTAL

Raw Materials

Polymer substrate in this work consists of three components, EP resin (EP51, Epoxide value: 0.48–0.54), curing agent (2-ethyl-4-methylimidazole) and diluent (Glycidyl methacrylate) at ratio of 100 : 5 : 10 by weight. All these components are supplied by Bailing Petrochemical, China. Carbon fiber used in the paper is T300B and supplied by TORAY Japan. Silver nitrate ($AgNO_3$), HCl (36% hydrochloric acid), sodium hydroxide (NaOH), ammonia ($NH_3{\cdot}H_2O$), stannous chloride ($SnCl_2$), palladium dichloride ($PdCl_2$) and alcohol are provided by Shanghai Dafeng Chemical Industry (China) and used as received without further purification.

Preparation of APCF

The preparation of APCF involved an initial pretreatment of CF, which included oxidization, sensitization and activation, and a subsequent reduction of $AgNO_3$ in the presence of HCHO.

CF (1 g) was oxidized in a solution of NaOH (2.5 mol/L, 200 mL) at 30°C for 2 h to improve its surface condition. After rinsing in deionized water, surface sensitization of CF was performed by immersion into an aqueous solution (70 mL) consisting of $SnCl_2$ (0.05 mol/L) and HCl (0.6 mol/L) at room temperature for 1 h. The surface activation of CF was conducted in an activator solution (50 mL) with $PdCl_2$ (0.003 mol/L), H_3BO (0.4 mol/L) and HCl (0.6 mol/L) at room temperature for 1 h. The treated CF was thoroughly rinsed in deionized water and dried completely at 110°C.

Finally, the treated CF was immersed into 100 mL HCHO (0.5 mol/L) solution with addition of appropriate drops of the $AgNO_3$ ammonia solution (100 mL) containing 68 g/L $AgNO_3$, 28g/L $NH_3{\cdot}2H_2O$, and stirred for 1 h. After washing and drying, Ag-plating CF was obtained. Illustration of APCF preparation is available in Supporting Information Figure S1.

Preparation of APCF-EP Composites

Epoxy resin, curing agent and diluent were admixed together at the weight ratio of 100 : 5 : 10. APCF was added into the mixture, and stirred until homogenously distribution. The APCF-resin mixture was poured into a mould under vacuum at 45°C, 2 h to remove the air. When APCF content more than 3 wt %, the mixture with high viscosity should be mechanically pressed

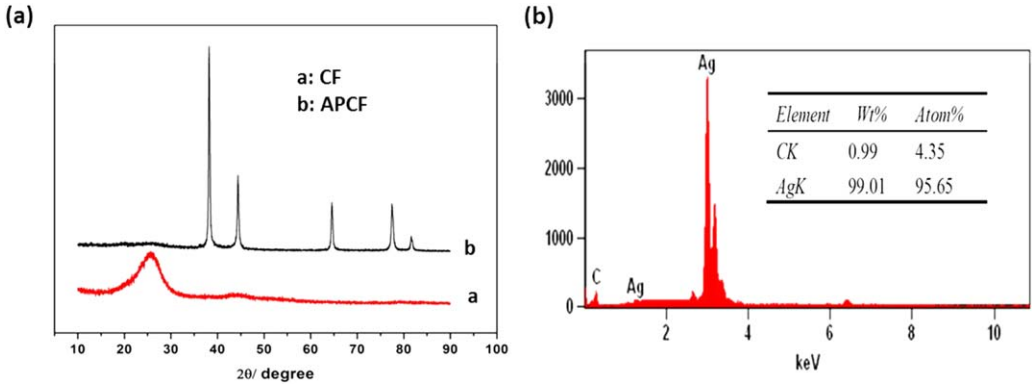

Figure 2. (a) XRD patterns of CF and APCF; (b) EDS spectrum of APCF. [Color figure can be viewed in the online issue, which is available at wileyonlinelibrary.com.]

to remove air bubbles inside. The resulting composite was further cured under vacuum at 80°C, 5 h.

Characterization

The morphologies and elementary analysis of CF, APCF and composites are characterized using a scanning electron microscope (SEM: AMRAY 100B model, USA) equipped with an energy dispersive X-ray spectroscopy (EDS) system.

The coating structures of APCF are detected by X-ray power diffraction (XRD: X'Pert Pro model, Holland).

The volume resistivity (ρ_v) and surface resistivity (ρ_s) are measured on a ZC-36 ultrahigh electric resistance meter (Shanghai, China) according to GB/T 1410-2006.

Flexural strength and impact strength of composites are measured by flexural strength testing machine(CMT-8502 model, Shengzhen Sansi) according to GB/T 9341-2000, and impact strength testing machine(BC-50 model, ShengZhen Sansi) according to GB/T 1043-1993, respectively.

Thermogravimetric analysis (TGA) curve is recorded using TA Q600SDT (TA Instrument, USA) from room temperature to 800°C at heating rate of 10°C/min in nitrogen atmosphere.

DSC curve is obtained by differential scanning calorimeter (PerkinElmer Inc., UK) from room temperature to 700°C at heating rate of 10°C/min in nitrogen atmosphere.

The measurement of thermal conductivity is conducted on Netzsch system (LFA427 German) at room temperature.

EMI shielding parameters of APCF-CF composite are analyzed by using an Agilent vector network analyzer in the frequency range of 8.2–12.4 GHz (X band). The vector network analyzer sends a signal down the waveguide upon a sample and the scattering parameter is gained to calculate the EMI shielding effectiveness (SE_{total}, SE_R, SE_A). All samples with a size of 10 mm diameter and 2.5 mm thickness.

RESULT AND DISCUSSION

Characterization of APCF and APCF-EP Composites

APCF was prepared by electroless plating, which transferred Ag produced by reduction reaction from solution to CF surface. Detail information about the APCF preparation is shown in Experimental. Figure 1(a) shows CF with an average length of 200 μm and diameter of 4–6 μm. The Ag coating on CF surface was dense and uniform. No void was observed in Figure 1(c). The thickness of Ag coating was estimated around 450 nm from the cross-sectional image of APCF in Figure 1(d).

The XRD patterns of CF and APCF are shown in Figure 2(a). The characteristic diffraction peaks appeared in the $2\theta = 38.22°$, 44.4°, 64.56°, 77.44°, and 81.6° corresponding to the (111), (200), (220), (311), and (222) planes, which can be indexed to the face-centered cubic structure of Ag. The oxidation state of Ag was not detected in the deposit coating. In addition, the XRD pattern showing a relatively narrow diffraction peak indicated the size of Ag crystallites was relatively small. The CF diffraction peak appeared in the $2\theta = 25.56$. However, it was flat and could not be seen in APCF pattern, indicating CF surface was covered by Ag coating. According to the Debye-Scherrer equation,[19] the thickness of Ag particles calculated from the XRD data was 0.457 μm, which coincides with the estimation by SEM image of cross-section in Figure 1(d).

Figure 2(b) shows the EDS of the APCF. Ag element peak appeared on the element map largely. A tiny carbon element peak indicated the coating on CF surface was almost Ag. The embedded table presents Ag atom and Ag mass fraction on the CF surface reached 95.65% and 99.01%, respectively. No Ag oxide phase was detected, which is consistent with the result of XRD.

The cross-sectional APCF-EP composite (3 wt % loading content) is shown in Figure 3(a). The bright parts and the dark parts are APCF and EP matrix, respectively. APCF was homogenously dispersed into EP substrate by random orientation without aggregation, which benefits uniformly thermal conduction along the heat flux direction.

Thermal and Electrical Conductivity of APCF–EP Composites

The thermally conductivity of composites filled with CF and APCF are shown in Figure 4(a). As shown the two curves give birth to the same tendency as filler content increasing, and a low percolation threshold of 1.6 wt %. When the loading content less than 1.6 wt %, thermal conductivities of their relative composites increased slowly due to the large interfacial thermal resistance between each fillers surrounded by a thick layer of

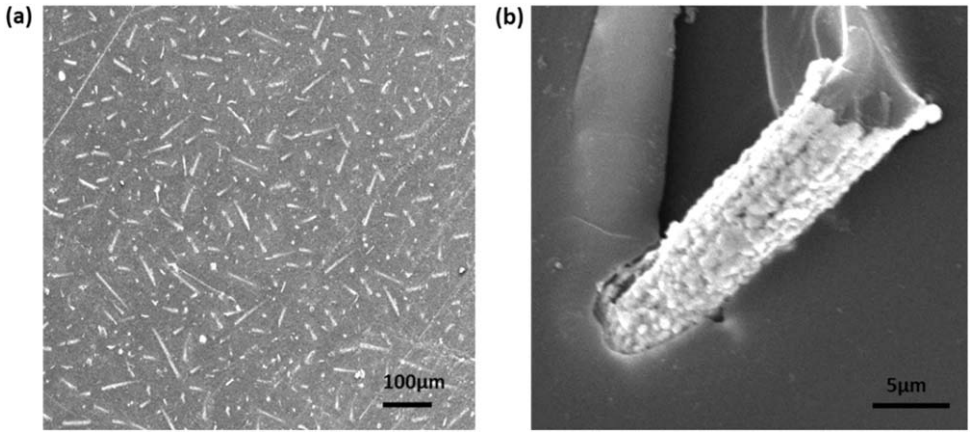

Figure 3. (a) Cross-sectional APCF-EP composite and (b) single APCF embedded into EP substrate.

polymer matrix. By increasing loading content until 4.5 wt %, thermal conductivities increased dramatically, thanks to the formation of a conductive interconnected network in the insulating polymer substrate. Heat could transfer along the thermally conductive network with lower heat resistance than that of EP polymer. Thermal conductivities of composites with more than 4.5 wt % loading content increased slowly, meaning thermally conductive paths tended to be temporarily saturated.

It's known that heat transportation in polymers by phonons, quantized models of vibration°C curring in a rigid crystal lattice, which are the primary mechanism since free movement of electrons is not possible.[6] EP substrate as an amorphous polymer possesses its thermal conductivity as low as to 0.2 W/m·K due to phonon scattering from numerous crystal defects. Ag exhibits excellent heat transportation by free electrons. At the same loading content, APCF–EP composites performed higher thermal conductivity than CF–EP composites due to the thin Ag coating on CF surface. At a loading content of 4.5 wt %, the thermal conductivity of APCF–EP composite increased to 2.33 W/m·K, which is approximately 2.6 times and 12 times higher than CF–EP composite and EP polymer, respectively. The thermal conductivity of APCF–EP composite increased to 2.49 W/m·K with a loading content up to 7 wt %. In previous reports, an EP composite with 10 wt % graphene flakes yielded only 1.53 W/m·K thermal conductivity.[4] A polyurethane–MWCNTs composite had a thermal conductivity of 0.47 W/m·K with a filling content of 3 wt %.[23]

The electrical conductivity of APCF–EP and CF–EP composites with loading content up to 7 wt % was measured in Figure 4(b). Compared with CF–EP composites, APCF–EP composites had low volume resistivity (ρ_v) and surface resistivity (ρ_s) due to high surface conductivity of APCF. As filler content increasing, volume resistivity (ρ_v) and surface resistivity (ρ_s) decreased from 1.7×10^{16} Ω·cm and 6.9×10^{15} Ω to 9.5×10^{3} Ω·cm and 6.2×10^{2} Ω, respectively, which approached the conductivity of metal.

EMI Shielding Effectiveness

EMI SE of a material is defined as the ratio between the incoming power and outgoing power of an electromagnetic wave, which is expressed in decibels (dB). The higher the SE value, the less electromagnetic energy passes through the materials.

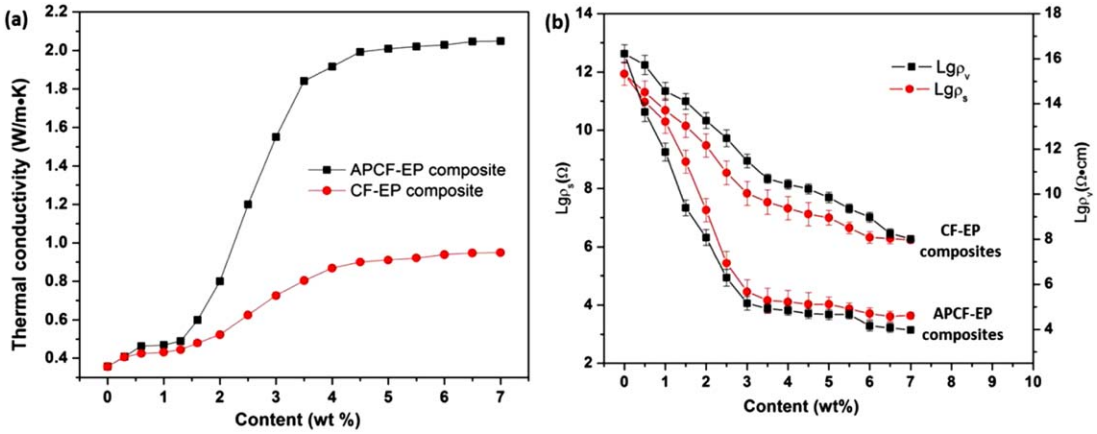

Figure 4. (a) Thermal conductivity of APCF-EP composites and CF-EP composites. Filling contents in both composites increased up to 7 wt %; (b) volume resistivity (ρ_v) and surface resistivity (ρ_s) of APCF-EP composites and CF–EP composites. [Color figure can be viewed in the online issue, which is available at wileyonlinelibrary.com.]

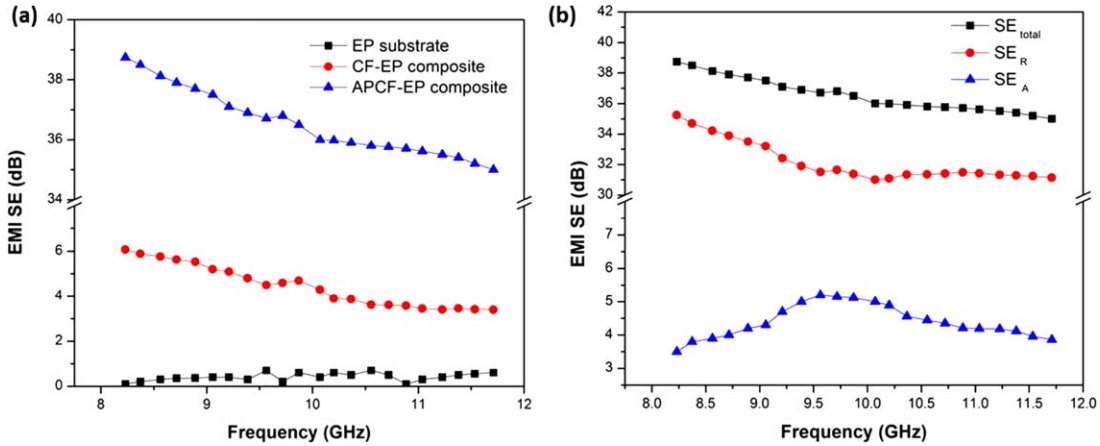

Figure 5. (a) EMI SE of EP substrate and its composites with 4.5 wt % APCF and 4.5 wt % CF, respectively, in the range of 8.2–12.4 GHz. (b) EMI SE (SE_{total}), microwave absorption (SE_A), and microwave reflection (SE_R) of EP composite with 4.5 wt % APCF. [Color figure can be viewed in the online issue, which is available at wileyonlinelibrary.com.]

EMI SE of APCF–EP composites with 4.5 wt % APCF as a function of frequency is shown in Figure 5(a). It can be seen that APCF–EP composites had SE of 38 - 35 dB in a frequency range of 8.2–12.4 GHz (X band), indicating that above 99.9% of the radiation was attenuated. According to the Schelkunoff theory, higher conductivity results in better ability to shield electromagnetic wave.[24] Due to the high electrical conductivity provided by APCF, APCF–EP composites exhibited higher EMI SE than CF–EP composites with less than 6 dB at the range of 8.2–12.4 GHz. EP substrate was obviously transparent to electromagnetic waves and exhibited almost no shielding ability. Compared with previous reports, it has been demonstrated that 7 wt % multi-walled CNTs[25] or 15 wt % single-walled CNTs[15] are required to approach the target value of the EMI SE needed for commercial applications around 20 dB. The APCF–EP composite performed much better EMI SE than commercial products.

The EMI shielding mechanism of APCF–EP composite was analyzed in Figure 5(b). When an electromagnetic wave is incident on a shielding material, the incident power is divided into reflected power, absorbed power and transmitted power. The power coefficients of reflectivity (R), transmissivity (T) and absorptivity (A) can be obtained from the measured scattering parameters (see Experimental). The relationship of the SE parameters is described as $R+T+A=1$. SE_{total}, SE_R and SE_A can be calculated as follows: $SE_{total}=-10\log T$, $SE_R=-10\log(1-R)$, $SE_A=SE_{total}-SE_R-SE_M$, where SE_M is the microwave multiple internal reflections, which is generally neglected when $SE_{total}>15$ dB.[26] Figure 5(a) shows SE_{total}, SE_R and SE_A of the APCF–EP composite as a function of frequency from 8.2 to 12.4 GHz. Obviously, the APCF–EP composite is both reflective and absorptive to electromagnetic radiation in the X-band frequency range, and reflection is the dominant shielding mechanism.

Mechanical Characterization

Mechanical strength of APCF–EP composites with various loading content is shown in Figure 6. With APCF increasing, both impact strength and flexible strength increased dramatically. As loading content up to 7 wt %, impact strength and flexural strength increased to 67 KJ/m^2 and 138.56 MPa, respectively. Mechanical properties of the composites depended upon APCF, which could prevent tiny crack initiation and propagation in EP substrate when external force applied.

Thermal Stability of APCF–EP Composites

The thermal stability of polymer composites largely depends on the polymer substrate. However, new characteristics may present due to the addition of fillers. The DSC as well as thermogravimetric results under nitrogen are shown in Figure 7(a,b), respectively. DSC curve shows T_g (glass transition temperature) of EP polymer is 120°C, indicative of beginning of EP polymer chain movement. T_g values of composites filled with 4.5 wt % and 7 wt % increased to 125°C and 135°C, respectively, meaning between APCF surface and EP substrate there was chemical bonding, such as hydrogen bond hindering the polymer chain movement, which improved T_g. Figure 7(b) shows EP substrate and composites started to degrade around 350°C due to polymer chain scission. Continuous weight loss of thermal

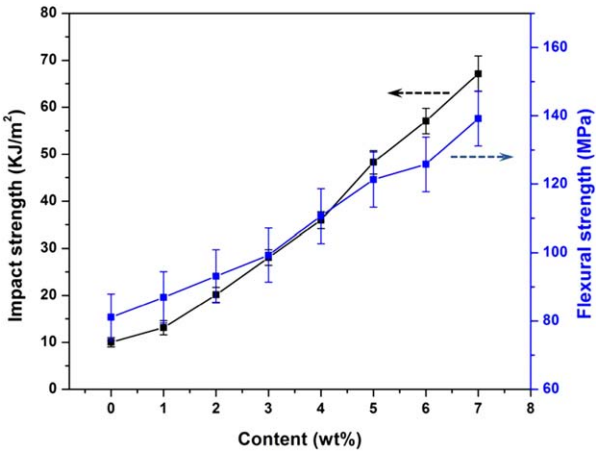

Figure 6. Mechanical properties of APCF–EP composites versus various loading contents. [Color figure can be viewed in the online issue, which is available at wileyonlinelibrary.com.]

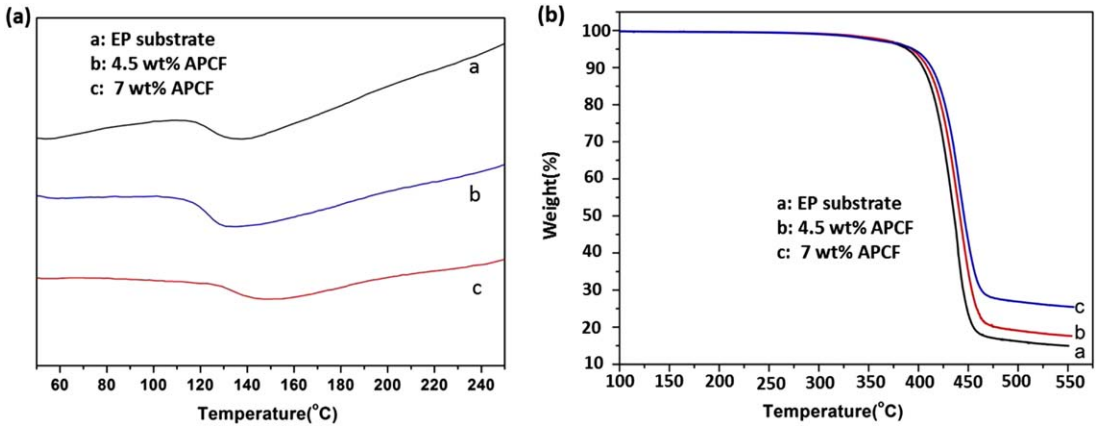

Figure 7. (a) DSC and (b) TG curves of EP substrate, composites with 4.5 wt % APCF and 7 wt % APCF, respectively. [Color figure can be viewed in the online issue, which is available at wileyonlinelibrary.com.]

decomposition of EP substrate and composites was observed until 470°C. The composites with loading content of 7 wt % and 4.5 wt % have 26% and 19% residue at 480°C, respectively, compared with 15% residue of EP substrate. In this way, it indicated APCF as an additive can improve thermal stability significantly.

CONCLUSION

In summary, we have fabricated a thermally conductive and electromagnetic shielding APCF–EP composite. APCF as conductive filler was prepared by electroless Ag-plating processing on the surface of CF with an average length of 200 μm. Ag layer around 450 nm thick was coating on the CF surface without Ag oxide phase detected in XRD and EDS spectrum. The APCF–EP composite with 4.5 wt % loading had thermal conductivity of 2.332 W/m·K, which is approximately 2.5 times higher than that of CF–EP composite at the same loading. As the loading content increasing to 7 wt % volume resistivity (ρ_v) and surface resistivity (ρ_s) decreased to 9.5 $\times$ 10^3 Ω·cm and 6.2 $\times$ 10^2 Ω, respectively, as well as mechanical properties and thermal stability were improved greatly. APCF–EP composite with 4.5 wt % loading performed EMI SE of 38–35 dB at frequency ranging from 8.2 to 12.4 GHz (X band), electromagnetic reflection was the dominant shielding mechanism. All performances indicate the APCF–EP composite can be applied commercially as lightweight thermally conductive and EMI shielding materials for electronic packing.

REFERENCES

1. Lin, W.; Moon, K.; Wong, C. P. *Adv. Mater.* **2009**, *21*, 2421.
2. Mamunya, Y.; Boudenne, A.; Lebovka, N.; Ibos, L.; Candau, Y.; Lisunova, M. *Compos. Sci. Technol.* **2008**, *68*, 1981.
3. Im, H., Kim, *J. Carbon* **2012**, *50*, 5429.
4. Song, S. H.; Park, K. H.; Kim, B. H.; Choi, Y. W.; Jun, G. H.; Lee, D. J.; Kong, B.; Paik, K.; Jeon, S. *Adv. Mater.* **2013**, *25*, 732.
5. Zhu, H.; Li, Y.; Fang, Z.; Xu, J.; Cao, F.; Wan, J.; Preston, C.; Yang, B.; Hu, L. *ACS Nano* **2014**, *8*, 3606.
6. Han, Z.; Fina, A. *Prog. Polym. Sci.* **2011**, *36*, 914.
7. Potts, J. R.; Dreyer, D. R.; Bielawski, C. W.; Ruoff, R. S. *Polymer* **2011**, *52*, 5.
8. Huang, X.; Iizuka, T.; Jiang, P.; Ohki, Y.; Tanaka, T. *J. Phys. Chem. C* **2012**, *116*, 13629.
9. Huang, X.; Zhi, C.; Jiang, P.; Golberg, D.; Bando, Y.; Tanaka, T. *Adv. Funct. Mater.* **2013**, *23*, 1824.
10. Weidenfeller, B.; Hofer, M.; Schilling, F. R. *Compos. A* **2004**, *35*, 423.
11. Zhou, M.; Lin, T.; Huang, F.; Zhong, Y.; Wang, Z.; Tang, Y.; Bi, H.; Wan, D.; Lin, *J. Adv. Funct. Mater.* **2013**, *23*, 2263.
12. Yu, A.; Ramesh, P.; Itkis, M. E.; Bekyarova, E.; Haddon, R. C. *J. Phys. Chem. C* **2007**, *111*, 7565.
13. Yu, A.; Ramesh, P.; Sun, X.; Bekyarova, E.; Itkis, M. E.; Haddon, R. C. *Adv. Mater.* **2008**, *20*, 4740.
14. Thomassin, J.; Pagnoulle, C.; Bednarz, L.; Huynen, I.; Jerome, R.; Detrembleur, C. *J. Mater. Chem.* **2008**, *18*, 792.
15. Li, N.; Huang, Y.; Du, F.; He, X. B.; Lin, X.; Gao, H. J.; Ma, Y. F.; Li, F. F.; Chen, Y. S.; Eklund, P. C. *Nano Lett.* **2006**, *6*, 1141.
16. AGARI; Y.; UEDA; A.; NAGAI; S. *J. Appl. Polym. Sci.* **1991**, *43*, 1117.
17. Wu, H.; Drzal, L. T. *Carbon* **2012**, *50*, 1135.
18. Li, L.; Yu, D.; Wang, L.; Wang, W. *J. Appl. Polym. Sci.* **2012**, *124*, 1912.
19. Zhang, Y.; Qi, S.; Wu, X.; Duan, G. *Synth. Met.* **2011**, *161*, 516.
20. Radke, A.; Gissibl, T.; Klotzbuecher, T.; Braun, P. V.; Giessen, H. *Adv. Mater.* **2011**, *23*, 3018.
21. Muench, F.; Rauber, M.; Stegmann, C.; Lauterbach, S.; Kunz, U.; Kleebe, H.; Ensinger, W. *Nanotechnology* **2011**, *22*.
22. Ma, Y.; Zhang, Q. *Appl. Surf. Sci.* **2012**, *258*, 7774.
23. Cai, D.; Song, M. *Carbon* **2008**, *46*, 2107.
24. Lu, Y.; Xue, L. *Compos. Sci. Technol.* **2012**, *72*, 828.
25. Yang, Y. L.; Gupta, M. C. *Nano Lett.* **2005**, *5*, 2131.
26. Yan, D.; Ren, P.; Pang, H.; Fu, Q.; Yang, M.; Li, Z. *J. Mater. Chem.* **2012**, *22*, 18772.